

## SUPPORTING INFORMATION

### Multi-scale time-resolved study of photoactivated dynamics in 5BenzylUracil, a model for DNA/protein interactions

Mohammadhassan Valadan,<sup>a</sup> Enrico Pomarico,<sup>b</sup> Bartolomeo Della Ventura,<sup>a</sup> Felice Gesuele,<sup>a</sup> Raffaele Velotta,<sup>a</sup> Angela Amoresano,<sup>c</sup> Gabriella Pinto,<sup>c</sup> Majed Chergui,<sup>\*b</sup> Roberto Improta,<sup>\*d</sup> and Carlo Altucci<sup>\*a</sup>

<sup>a</sup> Department of Physics "Ettore Pancini", University of Naples "Federico II", Naples, 80126, Italy. E-mail: carlo.altucci@unina.it

<sup>b</sup> Laboratory of Ultrafast Spectroscopy, ISIC, and Lausanne Centre for Ultrafast Science (LACUS), Ecole Polytechnique Fédérale de Lausanne, CH-1015 Lausanne, Switzerland. E-mail: majed.chergui@epfl.ch

<sup>c</sup> Chemical Sciences Department, University of Naples "Federico II", Naples, 80126, Italy.

<sup>d</sup> Institute for Biostructures and Bioimaging (IBB-CNR), Naples, Italy. E-mail: robimp@unina.it

#### Material and methods

##### Time-resolved fluorescence measurements on 5BenzylUracil

Samples are prepared with 30 mg of 5BenzylUracil (purchased from "Alchemy Srl" as a custom product) dissolved in 80 mL of methanol, showing an absorbance of approximately 0.3 at 266 nm, which falls within the lowest absorption band of 5BenzylUracil (5BU), in a 0.2 mm thick flow cell. Measurements are always performed on fresh samples and last no longer than 2 hours to avoid samples damage during the measurements, due to photocyclization of 5BU into 5,6BU.<sup>1</sup> We carefully make sure that photocyclization of the target is negligible in our experiment. In fact, the average power of the excitation beam is 3.5 mW; therefore in 2 hours, we deliver 25.2 J to the sample, that amounts to  $3.4 \cdot 10^{19}$  photons of 4.66 eV each. The absorbance of 0.3 implies:

$$\frac{I_{out}}{I_{in}} = 10^{-0.3} = 0.5$$

where  $I_{out}$  and  $I_{in}$  are the the intensity outgoing and incoming the target, respectively. Thus, the number of photoexcited molecules is  $1.7 \cdot 10^{19}$ , i.e. just half the overall number of incoming photons. The photocyclization quantum yield of 5BU is  $\approx 1.5 \cdot 10^{-3}$  what yields the number of photocyclized molecules is  $1.7 \cdot 1.5 \cdot 10^{16} \approx 2.5 \cdot 10^{16}$ , which is approximately 0.03% of the overall 5BU molecules we have in the sample in our concentration condition.<sup>2</sup> To corroborate our estimation and rule out any contribution of photocyclized product to the detected emitted signal we check static absorption spectra as well as the Total Ion Current (TIC) LC-MS/MS chromatograms of sample before and after the measurement. In fact, it is known that 5,6BU molecules do not significantly absorb at 250-260 nm.<sup>2</sup> Thus by checking that the static absorption spectrum of

target is unaffected by the FIUC measurement in the above spectral range we can safely infer that photocyclization is negligible. As a further proof of this we measured the TIC signal of the targets in LC-MS/MS diagnostics before and after a FIUC measurement to be essentially the same, whereas the TIC signal of heavily irradiated targets, exposed in separate session to about 100-300 times higher energy dose than that typical of the FIUC measurement, shows the appearance of another peak at earlier times as the signature of the formation of the photocyclized species. These results are reported in Figure S1 for the static absorption spectra (a) and for the TIC signal (b) and (c).

We also carry on another important optical check by experimentally estimating the fluorescence quantum yield of 5BU in methanol in comparison with that of a reference molecule such as tryptophan, finding a value of  $\approx 10^{-4}$ .

Ns-resolved fluorescence measurements are performed with a Time Correlated Single Photon Counting (TCSPC) system. The sample is pumped with 266 nm pulses at 150 kHz repetition rate, obtained by frequency tripling 80 fs pulses at 800 nm provided by a Coherent-Rega Ti: Sapphire regenerative amplifier. The average power of the excitation beam is attenuated to reduce the detected count rate to approximately 1% of the repetition rate in order to avoid saturation effects (pile-up). In the TCSPC measurements the sample flows into a 0.5 mm thick quartz flow cell. The direction of the excitation beam forms an angle with the plane of the cell such that the reflected beam can be blocked and does not enter the monochromator. Detection is performed within a window of 50 ns with an Instrument Response Function (IRF) of around 190 ps.

Sub-ps resolved luminescence measurements are performed via fluorescence up-conversion (FIUC) in the UV.<sup>3</sup> In this case, light emitted by the sample, which is pumped by the same excitation source as for the TCSPC measurements and flows in

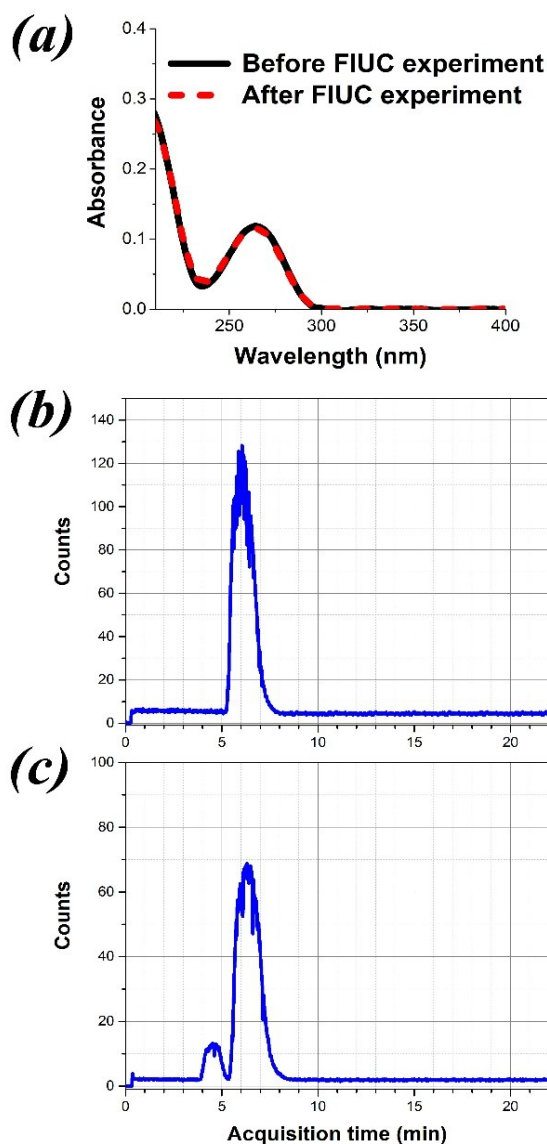


Fig. S1 (a) The static absorption spectra of 5BU sample before and after a FIUC experiment. (b) LC-MS/MS diagnostics before and after a FIUC measurement and (c) the LC-MS/MS signal of heavily irradiated target containing 5,6BU.

a 0.2 mm thick quartz flow cell, is collected by a parabolic mirror in forward-scattering geometry and then focused with a second parabolic mirror onto a Type I  $\beta$ -Barium Borate (BBO) crystal. The luminescence is then up-converted by mixing with the 800 nm gate pulse in a slightly non-collinear geometry. The up-converted signal is spatially filtered and detected via a liquid nitrogen-cooled CCD (charge-coupled device) camera after a spectrograph. By delaying the gate beam with respect to the onset of the fluorescence, while keeping the BBO crystal at a given angle, one can measure the kinetics of the emitted signal at a specific wavelength. Polychromatic detection is instead obtained by rotating the BBO crystal by a computer-controlled motor during the accumulation time of the CCD camera, so as to phase-match a wide spectral region at each time delay. Wavelength – time delay (2D) plots in the UV region (280 nm – 390 nm) can be obtained by rotating the BBO crystal at different

time delays. The IRF of the FIUC system (300 fs) is determined by measuring the temporal evolution of the Raman signal scattered from the solvent.

#### Computational details

Our computational analysis is based on CAM-B3LYP<sup>4</sup> and M052X<sup>5</sup> functionals. CAM-B3LYP is a long-range corrected functional, which has been tailored in order to accurately treat long-range Charge Transfer (CT) transitions. The M052X functional<sup>5</sup> which takes into account simultaneously exchange and correlation contributions, including kinetic energy and density, allows for a reliable treatment of dispersion interactions and, therefore, an accurate description of stacked systems. In contrast to “standard” functionals, both M052X and CAM-B3LYP provide a fairly accurate treatment of CT transitions, as shown by the fact that their predictions for oligonucleotides are in agreement with the available experimental results<sup>6</sup> and consistent with the findings of other wavefunction-based methods.

When applied to the study of photodimerization processes in DNA,<sup>7</sup> M052X provided a picture very similar to that obtained at the CASPT2 level<sup>8</sup> Geometry optimizations have been performed by using the 6-31+G(d,p) basis set, performing single point test calculations with the larger 6-311+G(2d,2p) basis set. When the excited state to be optimized crosses another excited state the optimization algorithm tries to follow the same diabatic states. In the presence of large mixings.

Solvent effects were included by using a mixed continuum/discrete approach. Bulk solvent effects have been computed by the polarizable continuum model (PCM),<sup>9</sup> while solute-solvent hydrogen bond interactions have been taken into account by explicitly including 2 CH<sub>3</sub>OH molecules in the adopted computational model. Based on our previous experience the energy of the  $n\pi^*$  transitions in pyrimidine is extremely sensitive to the inclusion of solute solvent hydrogen bonds. The starting coordination geometry of the two methanol molecules has been chosen in order to allow the formation of two OH---:O hydrogen bonds with the two carbonyl groups of BU, which are stronger than those formed by the amido hydrogen atoms and the oxygen Lone pairs of the methanol. Geometry optimization then leads to the coordination geometry shown in Figure SI4 or 6c in the main text, where one of the methanol molecules can form both OH---:O and an NH---:O hydrogen bonds, thus saturating simultaneously two potential HB sites of BU. We have performed test calculations considering the effect of an additional methanol molecule on the decay path of the bright excited state, which does not show any significant difference with respect the picture obtained with two methanol molecules.

We have exploited the “standard” linear-response (LR) implementation of PCM/TD DFT, for which analytic gradients are available.<sup>10</sup>

All the calculations were performed by the Gaussian09 Program.<sup>11</sup>

## Measurement of the 2D plot of 5BU with the FIUC set-up

A 2D plot of the fluorescence signal of 5BU in the range 280-390 nm has been measured with the FIUC set-up. The whole spectral range cannot be covered with a single measurement, because the detection in different UV spectral intervals requires different alignment conditions. Therefore, we divided the whole spectral range into two parts. The red region has been measured by blocking the excitation beam with a long pass filter at 290 nm, allowing one to reduce the background noise. The spectral response of the system in this spectral region is corrected by measuring the fluorescence of two reference organic dyes [2,5-diphenyloxazole (PPO) and para-terphenyl (PTP)] and by comparing their emission at long time delays with their steady-state fluorescence. In order to measure the blue region, no filter is used to block the pump, making the detection noisier than in the red part of the spectrum. The spectral response in this spectral range is corrected by measuring the fluorescence of another reference dye emitting more in the blue [1,2-diphenylacetylene (DPA)]. The measured 2D plots, where group velocity dispersion is separately corrected, are then connected at around 325 nm, where the two plots overlap.

### Analysis of the 2D plot

We performed a global fit on 17 kinetic traces extracted from the 2D plot. With this fitting procedure we impose for all traces a unique value for the time constants, but allow this value to vary.

The double exponential model provides the best fit of the data. In Fig. S2 the two decay associated spectra (DAS), that are the spectral distributions associated to the two time constants obtained from the global fit, are reported.

We find a time constant of  $(260 \pm 10)$  fs, which is present in the whole emission interval, and a second one of  $(1.31 \pm 0.2)$  ps, which characterizes in particular the red part of the covered spectral interval.

The obtained constants are in good agreement with the values of  $\tau_{2,310}$  and  $\tau_{2,350}$  determined with double exponential fits performed separately on the kinetic traces at 310 and 350 nm measured with long integration times. The first time constant ( $260 \pm 10$  fs) is slightly smaller than  $\tau_{1,310}$  and  $\tau_{1,350}$ . However, this discrepancy could be attributed to the noisier quality of the data in the blue part of the 2D plot. Moreover, as  $\tau_{1,310}$  and  $\tau_{1,350}$

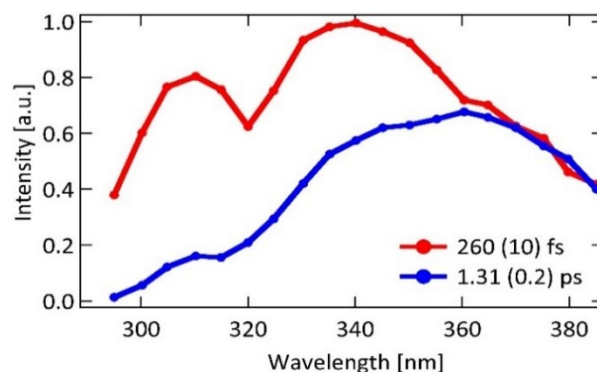


Fig. S2 DAS of the two time decay constants obtained with the global fit.

have similar value, the global fit is not able to distinguish between the two. The second time constant is in very good agreement with  $\tau_{2,310}$  and  $\tau_{2,350}$ . The DAS associated to the second time component shows a wide spectral distribution centered at around 350 nm, implying that the 1 ps time constant affects more the kinetics in the red part of the spectrum.

### 5BU fluorescence and concentration

We have investigated the dependence of the kinetics of the 5BU fluorescence on the sample concentration. In particular, we have measured the signal emitted at 310 nm and at 350 nm, corresponding to the two emission bands observed in the 2D plots described above, from 5BU samples with dilution factors of 10 and 100 with respect to the solution adopted in the previous up-conversion measurements (30 mg in 80 ml MeOH). These levels of dilution have been chosen in order to perform measurements with a reasonable S/N ratio.

In Fig. S3 the kinetic traces at both wavelengths for the samples with dilution factor 1, 10 and 100 are shown. At both wavelengths the dynamics does not change with the concentration.

A solution with dilution factor of 1000 has also been tested: in this case the kinetic traces at the two wavelengths (not reported in Fig. S3) are very noisy, especially the one at 310 nm, because of the very low level of detected signal. However, the traces even for such low concentrated solution essentially confirm the same dynamics. Furthermore, the signal emitted by the 5BU increases linearly with the concentration. These

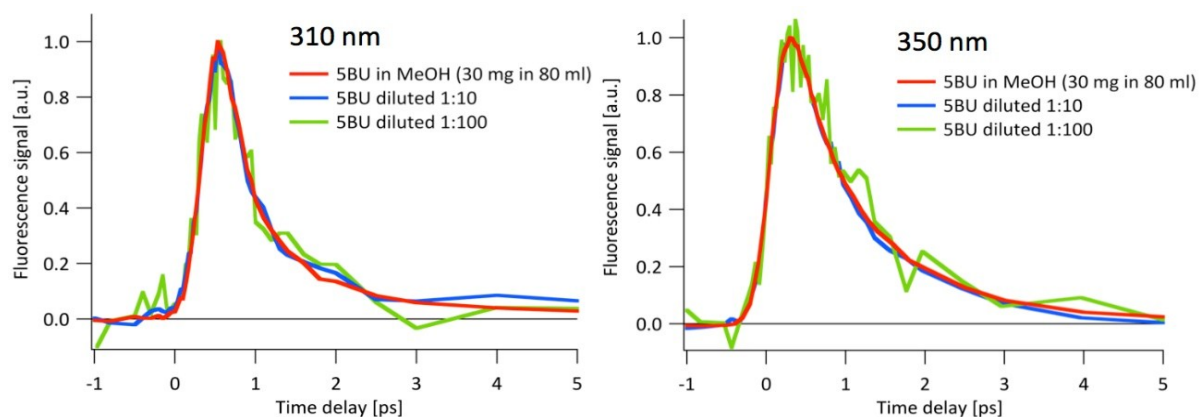


Fig. S3 Kinetic traces at 310 nm (left) and 350 nm (right) of the signal emitted by 5BU for dilution factors 1, 10 and 100.

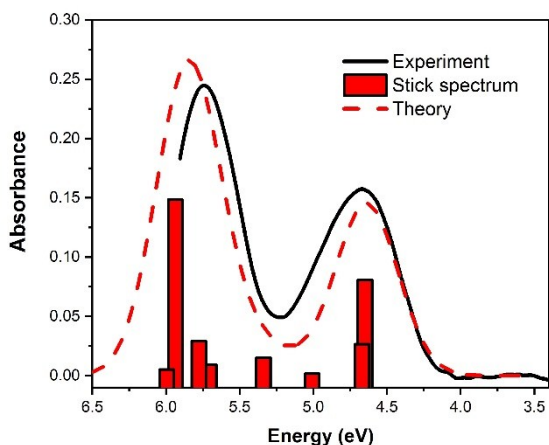


Fig. S4 Measured (Black solid line), and computed and corrected absorption spectra (Stick spectrum and Red dashes line) for 5BU in methanol solution.

results do not show aggregation effects at the first concentration we used; that would have produced a concentration-dependent dynamics or a nonlinear drop of the fluorescence signal. This point was also checked by mass spectrometry (see details below), where spectra obtained at different concentrations in 1:1000 overall concentration range were not significantly different, evidencing the presence of the only 5BU molecule and the absence of higher mass compounds.

## LC-MS analysis

The 5BU samples at different concentrations in 1:1000 overall concentration range were acidified by using 0.1% HCOOH before injecting to MS instrument. LC-MS was equipped by an Agilent HPLC system (1260 Series) on a reverse-phase C18 column (Agilent Life Sciences Poroshell 120 EC-C18, 2.1 x 100 mm, 2.7  $\mu\text{m}$ ) and coupled to an Agilent 6230 TOF mass spectrometer. The HPLC separation was carried out by using water and acetonitrile as mobile phases A and B, respectively. The injection volume was 20  $\mu\text{L}$  and a linear gradient was applied over 15 min run (0–5 min: 5% B, 5–10 min: 5–95% B, and further 5 min as a re-equilibration time) at a flow rate of 0.3 mL  $\text{min}^{-1}$ . The MS source was an electrospray ionization (ESI) interface in the positive ion mode with capillary voltage of 3000 V, gas temperature at 325  $^{\circ}\text{C}$ , dry gas ( $\text{N}_2$ ) flow at 5 L  $\text{min}^{-1}$  and the nebulizer at 35 psi. The MS spectra were acquired in a mass range of 150–1000  $m/z$  with a rate of 1 spectrum/s, time of 1000 ms/spectrum and transient/spectrum of 9961.

## Additional computational results

Measured and computed absorption spectra for 5BU in methanol solution are shown in Fig. S4. Molar extinction coefficients of 5BU at 266 nm is measured to be about 8100  $\text{L}\cdot\text{mol}^{-1}\cdot\text{cm}^{-1}$ . In order to simulate the computed spectrum each of the stick transitions is broadened by a Gaussian with Half Width at Half Maximum (HWHM) 0.25 eV.

The dominant contribution to the strong band at 5.8 eV comes from the lowest energy  $\pi$  orbital of the Ura ( $\text{U}\pi$ ) towards the second lowest energy  $\pi^*$  orbital of the pyrimidine ring (which would correspond to LUMO+1 in uracil). It is thus similar to the second absorption band found in Thymine and Uracil, though, also in this case, some participation of the benzene ring orbitals is found.

The relative energy of the ‘orthogonal’  $S_0$  minimum with respect to the absolute  $S_0$  minimum, according CAM-B3LYP and M052X functionals are reported in Table S1. The geometry optimization in methanol is performed at the PCM/6-31+G(d,p) level.

Functional	6-31+G(d,p)	6-311+G(2d,2p)
CAMB3LYP	0.03	0.03
M052X	0.05	0.05

Table S1 relative energy (in eV) of the ‘orthogonal’  $S_0$  minimum with respect to the absolute  $S_0$  minimum

## Excited state geometry optimizations

For orthogonal arrangements, after photoexcitation, CAM-B3LYP geometry optimizations of  $\text{U}\pi\pi^*$  predict that a steep path leads to a flat region of the Potential Energy Surface (PES), where the pyrimidine ring maintains a planar geometry, and the most significant geometry shifts mainly involve the bond lengths and bond angles of the ethylene-carbonyl moiety (O8C4C5C6 atoms). C4C5 distance decreases by 0.03  $\text{\AA}$ , C4O8 increases by 0.03  $\text{\AA}$ , and, especially, the C5C6 bond length increases by 0.1  $\text{\AA}$  in line with the bonding/antibonding character of HOMO and LUMO with respect to the C5C6 double bond. The energy gradient in this planar region is low (0.0005 a.u), suggesting that a part of the wavepacket could be dynamically trapped thereby, in agreement with what proposed for Ura and Thy.<sup>6, 13</sup> The oscillator strength is rather high (0.16) and the computed emission energy amounts to 4.35 eV ( $\lambda_{\text{corr}}=320$  nm). TD-CAM-B3LYP geometry optimization then leads to a non-planar minimum  $\text{U}\pi\pi^*$  ( $\text{U}\pi\pi^*\text{-min}$ ), where the pyrimidine ring takes a bent conformation (see Fig. 6a), with N3 and C6 out of the plane defined by N1, C2, C4, and C5 that are indeed close to being coplanar.  $\text{U}\pi\pi^*\text{-min}$  is only marginally more stable than the planar plateau (the energy difference 0.03 eV), but the emission from this minimum is remarkably red-shifted: 4.0 eV ( $\lambda_{\text{corr}}\sim 350$  nm).

M052X functional provides a similar picture, but for a slightly larger tendency to distort the ring planarity. The energy gradient at  $\text{U}\pi\pi^*\text{-pla}$  is larger than that found by CAM-B3LYP (0.002 a.u) and  $\text{U}\pi\pi^*\text{-min}$  is more stable than  $\text{U}\pi\pi^*\text{-pla}$  by  $\sim 0.10$  eV.

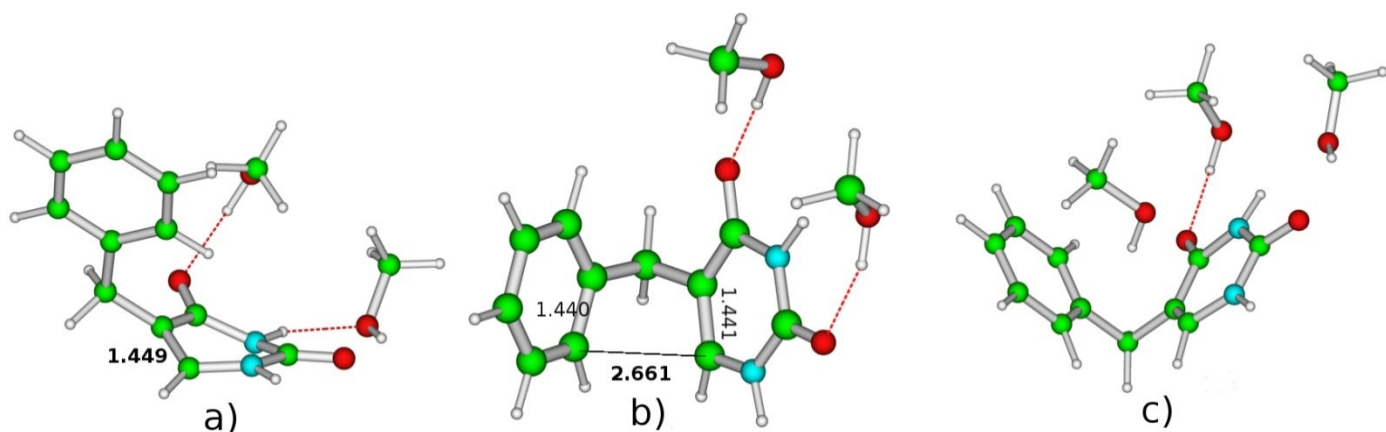


Fig. S5 Schematic drawing of  $\text{Ura}\pi\pi^*$ -min, the non-planar minimum of the lowest energy  $\pi\pi^*$  state localized on the Ura moiety (a) UB-exc-min, the exciplex minimum in the photochemical path (b) UB-exc-min, optimized by CAM-B3LYP for a model including two  $\text{CH}_3\text{OH}$  molecules (c) UB-exc-min, optimized by M052X for a model including three  $\text{CH}_3\text{OH}$  molecules.

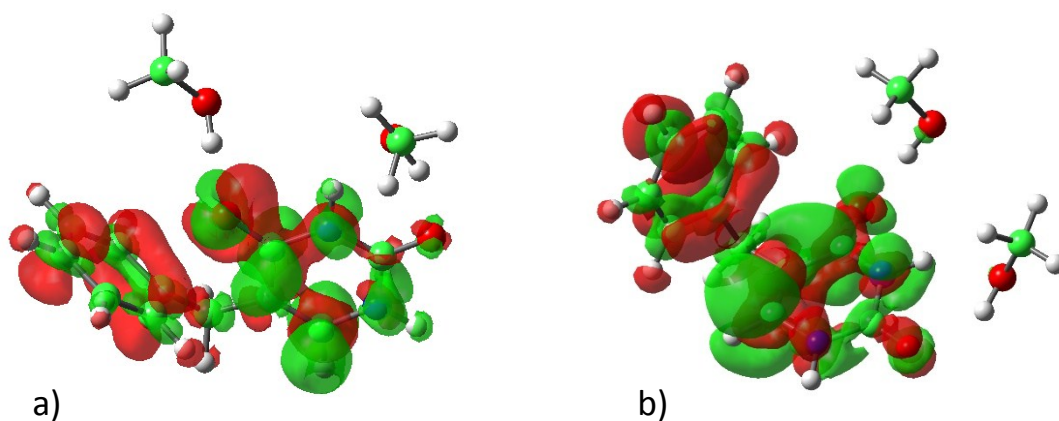


Fig. S6 Difference between the ground and the excited state density (a) in the minimum of the  $\text{Ura}\pi\text{CT}$  state (b) in UB-exc.

For what concerns the excited geometry optimizations starting from the FC region, for  $5\text{BU}\bullet 2\text{CH}_3\text{OH}$  M052X functional predicts barrierless decay to DIM-Cl\*. However, coordination of solvent molecules to the benzene ring, stabilized by dispersion interaction between the methyl group and the  $\pi$  aromatic ring, can make more difficult a closer approach of the ring and the decay to DIM-Cl\*. To check this point, we have performed some test-PCM/M052X/6-31+G(d,p) calculations considering three explicit  $\text{CH}_3\text{OH}$  molecules (see Fig. S6). In this case, our calculations predict the existence of the exciplex minimum, characterized by a C6-CB2 distance of 2.93 Å and by an emission energy at 357 nm (oscillator strength 0.07).

As anticipated in the main text, independently of the functional, geometry optimizations of  $S_2$  predict an increase of the mixing with the  $\text{B}^+ \rightarrow \text{U}^-$  CT state, as shown by the electron density difference depicted in Fig. 6. The involvement of the benzene moiety in the transition is clearly recognizable also in the geometry of  $\text{Ura}\pi\text{CT}$ -min. In the benzene moiety we observe indeed significant geometry shifts with respect to the FC point, with ring assuming a more quinoidal character, with a decrease of the CB2-CB3 and CB2'-CB3' bond lengths, and an increase of the other ones.  $\text{Ura}\pi\text{CT}$ -min. is characterized by a significant lengthening of the C4-O8 (up to 1.31 Å) bond length, and by a smaller increase of the C5C6 bond length, in line with the results obtained for the minimum of the  $\pi\pi^*$  state of Ura and Thy. On the other hand, for these two latter molecules both M052X and

CAMB3LYP predict the pyramidalization of C4 atom, whereas in  $\text{Ura}\pi\text{CT}$ -min the ring keeps a planar geometry.

## References

- 1 M. Micciarelli, M. Valadan, B. Della Ventura, G. Di Fabio, L. De Napoli, S. Bonella, U. Röthlisberger, I. Tavernelli, C. Altucci, R. Velotta, *J. Phys. Chem B*, **2014**, 118 (19), 4983-4992.
- 2 G. Sun, C. Fecko, R. Nicewonger, W. Webb, T. Begley, *Org. Lett.*; **2006**, 8 (4), 681-683.
- 3 A. Cannizzo, O. Bram, G. Zgrablic, A. Tortschanoff, A. A. Oskouei, F. van Mourik, M. Chergui, *Opt. Lett.* **2007**, 32 (24), 3555-3557.
- 4 T. Yanai, D. P. Tew, N. C. Handy, *Chem. Phys. Lett.* **2004**, 393, 51-57.
- 5 Y. Zhao, D. G. Truhlar, *Acc. Chem. Res.* **2008**, 41 (2), 157-167.
- 6 R. Improta, V. Barone, *Topics Curr. Chem.* **2014**, 355, 329-357.
- 7 (a) R. Improta, *J. Phys. Chem. B*, **2012**, 116 (49), 14261-14274. (b) L. Martínez-Fernández, R. Improta, *Photochem. Photobiol. Sci.* **2017**, 16 (8), 1277-1283 (c) I. Conti, L. Martínez-Fernández, L. Esposito, S. Hofinger, A. Nenov, M. Garavelli, R. Improta, *Chem. Eur. J.* **2017**, 23 (60), 15177-15188.
- 8 (a) L. Blancafort, A. Migani, *J. Am. Chem. Soc.* **2007**, 129 (47), 14540-14541. (b) J. J. Serrano-Perez, I. Gonzalez-Ramirez, P. B. Coto, M. Merchan, L. Serrano-Andres, *J. Phys. Chem. B*, **2008**, 112 (45), 14096-14098.
- 9 J. Tomasi, B. Mennucci, R. Cammi, *Chem. Rev.* **2005**, 105 (8), 2999-3094.
- 10 G. Scalmani, M. J. Frisch, B. Mennucci, J. Tomasi, R. Cammi, V. Barone, *J. Chem. Phys.* **2006**, 124, 094107.

- 11 M. J. Frisch, et al Gaussian 09, revision A.02; Gaussian Inc.: Wallingford CT, **2009**.
- 12 F. J. Avila Ferrer, J. Cerezo, E. Stendardo, R. Improta, F. Santoro, *J. Chem. Theory Comp.* **2013**, 9 (4), 2072-2082.
- 13 R. Improta, F. Santoro, L. Blancafort, *Chem. Rev.*, **2016**, 116 (6), 3540-3593.